Nuclear Physics A 697 (2002) 3–24
www.elsevier.com/locate/npe

Multiparticle excitations in ^{194}Pb

M. Kaci [a,b,*], M.-G. Porquet [a], I. Deloncle [a], M. Aiche [a,1], F. Azaiez [b], G. Bastin [a], C.W. Beausang [c,2], C. Bourgeois [b], R.M. Clark [d,3], R. Duffait [e], J. Duprat [b], B.J.P. Gall [a,4], F. Hannachi [a], K. Hauschild [d,5], M.J. Joyce [c,6], A. Korichi [b,a], Y. Le Coz [e,5], M. Meyer [e], E.S. Paul [c], N. Perrin [b], N. Poffé [f,b], N. Redon [e], C. Schück [a], H. Sergolle [b], J.F. Sharpey-Schafer [c,7], J. Simpson [g], A.G. Smith [h], R. Wadsworth [d]

[a] *CSNSM, IN2P3/CNRS and Université Paris-Sud, 91405 Orsay Campus, France*
[b] *IPN, IN2P3/CNRS and Université Paris-Sud, 91406 Orsay, France*
[c] *Oliver Lodge Laboratory, University of Liverpool, PO Box 147, Liverpool L69 3BX, UK*
[d] *University of York, Department of Physics, Helsington, York YO1 5DD, UK*
[e] *IPN, IN2P3/CNRS and Université C. Bernard Lyon-1, 69622 Villeurbanne, France*
[f] *University of Oxford, Department of Physics, Keble Road, Oxford OX1 3RH, UK*
[g] *Daresbury Laboratory, Daresbury, Warrington WA4 4AD, UK*
[h] *Schuster Laboratory, University of Manchester, Manchester M13 9PL, UK*

Received 31 January 2001; revised 28 May 2001; accepted 26 June 2001

Abstract

High-spin states of ^{194}Pb have been populated by the reaction ^{184}W(^{16}O, 6n) at 113 MeV beam energy and studied using the EUROGAM-1 array. The level scheme has been extended up to spin of $33\hbar$ and excitation energy of 11.1 MeV. The high-spin part of the level scheme is dominated by bands of dipole transitions. New dipole bands have been observed and the configurations of their band heads are discussed. Besides the well-known coupling of the $K^\pi = 11^-$ two-proton state to several $\nu i_{13/2}$ rotation-aligned neutron states, the $K^\pi = 8^+$ two-proton state is also involved. Such a coupling is identified for the first time in a lead isotope. Moreover, the $K^\pi = 11^-$ two-proton state is coupled to the rotation-aligned proton pair $(\pi h_{11/2})^2$. Thus many multiparticle configurations involving *all*

* Corresponding author. Present address: IFIC, Edificio Institutos de Paterna, Apartado 22085, 46071 Valencia, Spain.
E-mail address: kaci@evala4.ific.uv.es (M. Kaci).
[1] Present address: CENBG, IN2P3-CNRS, 33170 Gradignan, France.
[2] Present address: A.W. Wright Nuclear Structure Laboratory, New Haven, CT 06511, USA.
[3] Present address: Lawrence Berkeley Laboratory, Berkeley, 94720, USA.
[4] Present address: IReS, IN2P3-CNRS and Université Louis Pasteur, 67037 Strasbourg, France.
[5] Present address: DAPNIA, CEA, 91190 Gif-sur-Yvette, France.
[6] Present address: Research Laboratory, BNFL Springfields, Preston PR4 0XJ, UK.
[7] Present address: NAC, Faure PO Box 72, ZA 7131, South Africa.

PII: S0375-9474(01)01225-8

the high-j subshells located around the proton and neutron Fermi levels, $\pi h_{11/2}$, $\pi h_{9/2}$, $\pi i_{13/2}$, and $\nu i_{13/2}$ have been identified in this nucleus.

PACS: 23.20.Lv; 23.20.En; 27.80.+w
Keywords: NUCLEAR REACTIONS ^{184}W(^{16}O, 6n)^{194}Pb, $E = 113$ MeV; Measured E_γ, I_γ, angular distribution, γ–γ–γ-coinc, dipole bands, multiparticle configurations.^{194}Pb deduced levels, I^π, $B(\mathrm{M1})/B(\mathrm{E2})$ ratios; Compton-suppressed Ge-detector array.

1. Introduction

Because of their closed proton shell, $Z = 82$, the lead isotopes are well known to have a spherical shape in their ground state. Up to the spin value $I \approx 20\hbar$, most of the yrast states have been interpreted as pure neutron excitations involving the shell-model orbitals $\nu i_{13/2}$, $\nu p_{3/2}$ and/or $\nu f_{5/2}$ [1]. The study of the β-decay of the Bi isotopes [2] and the α-decay of the Po isotopes [3] has revealed the existence of excited states, $I^\pi = 0_2^+$, in the even-neutron deficient lead isotopes, $^{190–200}$Pb. These states have been interpreted as a two-proton–two-hole excitation across the shell gap, related to a weakly-deformed oblate shape [2]. Moreover, excited states, $I^\pi = 2_2^+$, have also been observed in $^{192–196}$Pb and interpreted as the first member of the rotational bands built on the $I^\pi = 0_2^+$ states [2]. Higher members, $I^\pi = 4^+$ and $I^\pi = 6^+$, have been identified in ^{196}Pb [4]. Two-proton excited states, $I^\pi = 8^+$ and $I^\pi = 11^-$, involving the high-K intruder orbitals corresponding to an oblate shape have been well identified in ^{192,194,196}Pb isotopes [4–6]. These states are isomeric and are located in all these nuclei at about the same excitation energy above the $I^\pi = 0_2^+$ states (around 1.5 MeV and 2.0 MeV, respectively). The measured value of the g-factor ($g = 0.96$) of the $I^\pi = 11^-$ state in ^{196}Pb is consistent with the excited two-proton configuration $\pi h_{9/2} i_{13/2}$ [4].

The high-spin level schemes of the lead isotopes with $A = 192$–202 [7] are dominated by many sequences of dipole transitions (measured M1 in ^{194}Pb [8], ^{195}Pb [9], ^{197}Pb [10], and ^{199}Pb [11]), which have been named “shears bands”, some of them being very regular in energy. The band heads have been interpreted as many-particle excitations, involving both proton and neutron excitations in the high-j subshells located around the Fermi levels. Proton excitations correspond to particles in the $\pi h_{9/2}$ and $\pi i_{13/2}$ subshells and neutron excitations to several holes in the $\nu i_{13/2}$ subshell, leading to the perpendicular coupling of the angular momenta of the protons and the neutrons.

It is interesting to note that such a coupling had been observed, many years ago, in several odd–odd $_{81}$Tl isotopes [12,13]. In this case, particle-rotor models can be used to describe the low-lying excited states [14,15]. The theoretical results are in good agreement with the experimental ones, particularly the spin value of the lowest states and the small transition energies of the low part of the bands. The $h_{9/2}$ proton and $i_{13/2}$ neutron are pointing perpendicular to each other with the resultant spin $I = 8$. This coupling scheme changes when going to higher spins, because of the continuous alignment of the angular momentum of the proton along the rotational axis (i.e., the total angular momentum, as the neutron angular momentum is yet aligned along the rotational axis). This gives the

$I = 8$–11 multiplet of states, lying close in energy [14]. The maximum spin obtained when the angular momenta of the odd neutron and odd proton are completely aligned is 11. From here on, the system gains angular momentum by collective rotation. The description of the dipole bands observed in lead isotopes, which cannot be done using such an approach because of the too large number of quasiparticles, has been extensively performed using the Tilted Axis Cranking (TAC) model [16]. It gives an analogous result, and suggests a gradual alignment of the proton and neutron spins into the direction of the total angular momentum. This behavior has been called "shears mechanism" since it resembles the closing of a pair of shears and is supported by the decrease of the experimental $B(\mathrm{M1})$ values along the bands [17]. Within this formalism, magnetic rotation has been suggested for these dipole bands [18]. More recently, another approach has been used considering residual interactions between neutrons and protons, leading to the rotational-like behaviour of the multiplet states [19].

In many cases, the dipole bands are not connected to the low-lying states and therefore their spin value and excitation energy are unknown, which prevents the precise identification of the neutron and the proton configurations involved in these high-spin high-energy states. In ^{194}Pb, the band heads of two dipole structures had been connected to the low-lying states [20], making this nucleus very attractive for further studies on dipole band heads and multiparticle identifications. The aim of the work presented in this paper is to enlarge the level scheme of this nucleus, in order to identify most of the multiparticle configurations involving *all* the high-j subshells located around the proton and neutron Fermi levels. By using the EUROGAM-1 array, the level scheme of ^{194}Pb has been extended to higher spin and higher excitation energy than previously known. Indeed the already known dipole bands [20–22] have been extended, several new structures have been observed and their decays have been measured. The structures of all the band heads are discussed, leading to a comprehensive interpretation of the whole multiparticle excitations involved in this nucleus at high spin.

In addition, it is worth noting that ^{194}Pb is one of the few nuclei where the yrast superdeformed band, which has been studied using the data from the present experiment [23], has finally been connected to the normal deformed states [24].

2. Experiment and results

High-spin states of ^{194}Pb have been populated by the ^{184}W(^{16}O, 6n) reaction at 113 MeV bombarding energy. The beam of ^{16}O was provided by the tandem accelerator at the Nuclear Structure Facility, Daresbury Laboratory. Two stacked 325 μg/cm^2 targets of enriched ^{184}W, each with a 10 μg/cm^2 carbon backing, were used. The γ-rays were detected with the EUROGAM-1 detector array consisting of 45 large volume Ge detectors placed in rings at angles $\theta = 72.05°$, 85.84°, 94.16°, 107.94°, 133.57°, and 157.60°, with respect to the beam direction. Compton-suppressed γ-ray coincidence events were recorded when at least 5 unsuppressed Ge detectors fired in prompt coincidence. A total of 860 million events were recorded on tapes, comprising 430 million three-fold, 280 million four-fold, 99 million five-fold and 21 million six-fold escape-suppressed events. In the off-line analysis, several gated γ–γ matrices with energy windows set on different yrast transitions were created. Moreover, multigated spectra have been built at each detection angle in order to analyze angular distributions [25].

The main exit channels of the reaction used in this experiment lead to ^{194}Pb and ^{195}Pb. The study of high-spin states of the latter nucleus has been already published elsewhere [26].

In thin target experiments, transitions above and below the long-lived isomers are not observed in coincidence, since the recoiling nuclei leave the focal volume of the Ge detectors. Thus, because of the presence of the two long-lived isomeric states, $I^\pi = 11^-$ ($T_{1/2} = 124$ ns) and $I^\pi = 12^+$ ($T_{1/2} = 350$ ns), the intensity of the $2^+ \rightarrow 0^+$ transition measured in this work is not representative of the total population of the ^{194}Pb nucleus in the reaction. From our previous experiment [20] where a backed target had been used to stop the recoiling nuclei, we have extracted the intensity corresponding to the prompt feeding of the ground state, 27%, when the rest of the total intensity is shared between the direct population of the long-lived isomers, 29% for the $I^\pi = 11^-$ state and 43% for the $I^\pi = 12^+$ state. Since the same relative population of the two long-lived isomeric states has been obtained in the present work, these three values have been used for the intensity normalization (see Table 1).

Table 1
Energy, intensity, angular distribution coefficient and multipolarity of the transitions in ^{194}Pb

	E_γ [a] (keV)	I_γ [a]	a_2 [a]	Multipolarity	I_{tot}
PART 1					
	(47) [b]				
	143.4 (3)	0.7 (2)	−0.13 (5)	M1	3.3
	166.1 (2)	4.9 (3)	0.20 (5)	E2	9
	173.7 (2)	2.9 (2)	−0.12 (5)	E1	3.2
	178.1 (2)	2.0 (5)	−0.08 (5)	M1	5.8
	196.4 (3)	1.4 (3)			
	197 (1)	0.3 (2)			
	(231) [d]				
	260.5 (3)	1.7 (2)	−0.15 (5)	M1	2.8
	280.1 (2)	20 (3)	−0.28 (5)	E1	21
	284.0 (2)	1.4 (4)	−0.34 (5)	M1	2.2
	294.6 (3)	0.3 (2)			
	302 (1)	1.8 (5)			
	(305) [d]				
	352 (1)	0.8 (2)			
	358.1 (3)	1.4 (3)			
	361.2 (3)	1.0 (3)			
	380.4 (3)	0.5 (2)			
	416.2 (4)	0.4 (2)			
	421.2 (2)	21 (3)	0.16 (5)	E2	22
	456 (1)	0.3 (1)			

Table 1 —continued

	E_γ [a] (keV)	I_γ [a]	a_2 [a]	Multipolarity	I_{tot}
	459.5 (2)	1.8 (2)			
	496 (1)	0.8 (3)		E3	0.8
	519.6 (2)	5.1 (5)	0.15 (5)	E2	5.2
	538.1 (2)	3.1 (4)	0.20 (5)	E2	3.2
	558.6 (3)	0.4 (1)			0.4
	575.1 (2)	25 (3)		E2	26
	577.9 (3)	4.2 (3)	0.12 (5)	E2	4.3
	587.0 (3)				
	595 (1)	4 (2)			4
	612 (1)	0.7 (3)			0.7
	627.9 (3)	0.9 (3)			0.9
	632.1 (3)	0.3 (1)			0.3
	672.3 (2)	2.5 (4)	0.12 (5)	E2	2.5
	705.4 (2)	1.4 (4)	0.14 (5)	E2	1.4
	767.9 (2)	0.9 (3)			0.9
	787.7 (2)	4.2 (2)	0.45 (5)	E2	4.2
	800.4 (2)	1.0 (3)			1.0
	863.9 (2)	4.5 (5)	0.16 (5)	E2	4.5
	(931) [d]				
	965.2 (2)			E2	**27** [e]
	1065.9 (3)	1.0 (5)			1.0
	(1309) [d]				
PART 2					
Band 1a	119.2 (2)	1.7 (5)	−0.38 (5)	M1	12
	144.7 (2)	2.9 (5)	−0.32 (5)	M1	13
	196.9 (2)	5 (1)	−0.38 (5)	M1	12
	260.1 (2)	6 (1)	−0.34 (5)	M1	10
	336.2 (2)	6 (1)	−0.38 (5)	M1	8
	375.5 (2)	5 (2)	−0.35 (5)	M1	6
	385 (1)	0.4 (2)			0.5
	417.1 (3)	2.1 (5)	−0.5 (1)	M1	2.5
	423.7 (3)	1.5 (5)	−0.4 (1)	M1	1.8
	428.2 (3)	0.7 (5)	−0.37 (5)	M1	0.8
	441.9 (2)	1.3 (5)	−0.35 (5)	M1	1.5
	711.7 (4)	0.6 (3)	0.27 (5)	E2	0.6
	793.3 (5)	0.5 (2)	0.4 (1)	E2	0.5
	(840) [c]				
Band 1b	129.0 (4)	0.7 (3)	−0.05 (5)	M1	4
	195.8 (2)		−0.19 (5)	M1	
	208.4 (2)	1.1 (3)	−0.23 (5)	M1	2.5
	269.4 (2)	2.2 (5)	−0.20 (5)	M1	3.5
	498.8 (3)	2.2 (5)	−0.6 (2)	M1	2.5
Band 1c	328.6 (2)	1.9 (3)	−0.39 (5)	M1	2.5
	363.5 (5)		−0.3 (1)	M1	
	372.8 (3)		−0.13 (5)	M1	
	387.8 (3)		−0.5 (1)	M1	
	396.6 (2)	1.7 (3)	−0.6 (1)	M1	2.0

Table 1 —continued

	E_γ [a] (keV)	I_γ [a]	a_2 [a]	Multipolarity	I_{tot}
Group A	(83)[b]				
	255.5 (3)				
	342.8 (2)				
	364 (1)		−0.3 (2)	M1	12
	514.8 (2)	26 (3)	−0.3 (1)	M1 + E2	26
	526.4 (2)				
	541.6 (2)		−0.5 (1)	M1 + E2	**14**[e]
	609.3 (2)	24 (2)	0.4 (1)	E2	24
	(869)[c]				
	890.6 (3)				
	906.0 (2)		0.4 (1)	E2	**15**[e]
PART 3					
Band 2a	130.1 (4)	1.2 (3)	−0.17 (5)	M1	7
	136.6 (4)	1.0 (5)	−0.11 (5)	M1	5
	162.9 (2)	3.2 (5)	−0.26 (5)	M1	11
	260.6 (2)	2.4 (5)	−0.22 (5)	M1	4
	303.2 (2)	8 (2)	−0.4 (1)	M1	12
	363 (1)	3.9 (6)	−0.3 (2)	M1	5
	376.4 (4)	6 (2)	−0.41 (5)	M1	8
	396.9 (2)	9 (2)	−0.40 (5)	M1	11
	700 (1)			E2	
	739.8 (3)	0.7 (2)		E2	0.7
	773.5 (3)	1.0 (5)	0.2 (1)	E2	1.0
Band 2b	212.2 (2)	1.7 (2)	−0.28 (5)	M1	3.6
	227.6 (2)	1.5 (2)	−0.33 (5)	M1	2.9
	267.3 (2)	1.5 (2)	−0.20 (5)	M1	2.5
	306.9 (2)	1.3 (3)	−0.4 (1)	M1	1.9
	361 (1)	1.3 (5)	−0.3 (2)	M1	1.4
	393.6 (3)	0.7 (2)	−0.4 (1)	M1	0.9
	420.9 (3)	0.6 (1)		(M1)	0.7
	440.9 (3)	0.3 (1)		(M1)	0.4
	462 (1)	0.2 (1)		(M1)	0.2
	484.2 (2)	0.06 (3)		(M1)	0.07
	505 (1)				
	(525)				
Band 2c	296.5 (2)				
	305.0 (2)				
	316.4 (3)		−0.38 (5)	M1	
	348.0 (3)	2.2 (4)	−0.34 (5)	M1	2.8
	350.6 (3)		−0.33 (5)	M1	
	409.4 (2)	2.8 (4)	−0.44 (5)	M1	3.3
	(699)[c]				
	(757)[c]				
Group B	(43)[b]				
	(64)[b]				
	140.1 (3)	[f]	−0.17 (5)	M1	

Table 1 —continued

	E_γ [a] (keV)	I_γ [a]	a_2 [a]	Multipolarity	I_{tot}
	351.8 (2)				
	464.7 (2)				
	488.4 (2)				
	493.2 (1)				
	506.8 (3)	0.6 (3)			0.7
	(534)				
	536.9 (2)	3.4 (5)	0.11 (5)	E1	3.5
	723.1 (3)				
	840.8 (2)				
	845.4 (2)				
	858.0 (2)	1.8 (5)	0.12 (5)	E1	1.8
	953.2 (2)		0.14 (5)	E2	
	(963) [c]				
	980.9 (2)				
	1028.3 (3)				
	1081.7 (5)	1.0 (4)			1.0
	1154.5 (5)				
	1302.5 (5)				
	1399.5 (5)				
	1687.5 (5)				
	1704.7 (8)				
PART 4					
Band 3	162.2 (2)	0.4 (1)		M1	1.5
	232.8 (2)	1.4 (4)	−0.35 (5)	M1	2.6
	287.9 (2)	1.7 (4)	−0.4 (1)	M1	2.6
	347.8 (2)	1.6 (3)	−0.4 (1)	M1	2.1
	361 (1)				
	374.3 (3)	1.0 (3)		M1	1.3
	377.5 (5)	0.3 (1)			
	396.9 (2)	0.6 (2)	−0.4 (1)	M1	0.7
	636.0 (3)	0.2 (1)		E2	0.2
	722.2 (3)	0.2 (1)		E2	0.2
	771.1 (3)	0.2 (1)		E2	0.2
Band 4	201.9 (3)	0.3 (1)			
	249.1 (2)	0.7 (2)	−0.24 (5)	M1	1.2
	276.3 (2)	0.6 (2)	−0.36 (5)	M1	1.0
	317.5 (2)	0.6 (2)	−0.4 (1)	M1	0.8
	363.1 (2)	0.5 (2)	−0.4 (1)	M1	0.6
	384.7 (2)	0.3 (1)	−0.5 (1)	M1	0.4
	412.5 (3)	0.25 (3)	−0.4 (1)	M1	0.3
Group C	255.7 (3)	0.2 (1)			
	273.0 (3)	0.5 (2)		M1	0.8
	341.7 (3)	0.2 (1)			
	461.8 (2)	2.7 (3)			
	568.0 (3)	0.5 (2)			0.5
	574.6 (2)	18 (3)	0.26 (5)	E2	18
	591.2 (2)	1.3 (2)	0.3 (1)	M1	1.4
	614.7 (3)	0.5 (2)	−0.3 (1)	M1	0.5

Table 1 —continued

	E_γ [a] (keV)	I_γ [a]	a_2 [a]	Multipolarity	I_{tot}
	659.5 (2)	10 (2)	0.26 (5)	E2	10
	677.4 (3)	0.6 (2)			0.6
	753.3 (2)	1.4 (2)	−0.34 (5)	M1	1.5
	755.0 (2)	3.7 (3)			3.7
	785.8 (4)	0.3 (2)			0.3
	819.9 (3)	0.8 (2)			0.8
	824.4 (2)	1.4 (2)			1.4
	892.7 (2)	2.0 (3)	−0.4 (1)	M1	2.1
	932.7 (2)			E2	**43**[e]
	962.9 (3)	0.9 (3)			0.9
	1007.0 (5)	0.5 (2)			0.5
	1165.6 (5)		0.3 (1)	E2	
Group D	158.1 (2)				
	(283)[c]				
	326.3 (2)	8 (1)	0.12 (5)	E2	9
	372.5 (2)	10 (2)	−0.37 (5)	M1	13
	376 (1)	1.9 (5)			
	441.6 (2)	22 (3)	−0.18 (5)	E1	22
	459.9 (2)	0.9 (3)			0.9
	473.5 (2)	0.7 (2)			0.7
	576 (1)	0.7 (3)			0.8
	581.1 (2)	1.7 (5)			1.7
	597.0 (2)	4.1 (5)			4.2
	613.0 (2)	1.8 (3)			1.8
	654.1 (2)	1.9 (2)			1.9
	696.7 (3)				
	714.9 (2)	1.4 (3)			1.5
	727.5 (2)	2.0 (3)			2.0
	758.3 (2)	1.0 (3)			1.0
	759.9 (2)	0.8 (3)			0.8
	817.6 (2)	0.4 (2)			0.4
	849.1 (3)	3.9 (5)	0.23 (5)	E2	4.0
	947.9 (2)	0.7 (4)			0.7
	1028.8 (3)	1.7 (6)	0.16 (5)	E2	1.7
	1056.9 (4)	1.5 (5)			1.5
	1058.8 (4)	0.5 (2)			0.5
	1123.3 (5)	0.3 (1)			0.3
	1215.5 (5)	0.3 (1)			0.3
	1241.5 (5)	0.6 (3)			0.6
	1310.8 (6)	0.2 (1)			0.2

[a] The number in parenthesis is the error in the last digit.
[b] Deduced from coincidence relationships.
[c] Tentative assignment.
[d] Observed in another work.
[e] Value used for intensity normalization (see text).
[f] Intensities of transitions belonging to group B, which can be determined only from spectra gated by transitions located above them, are given in Table 3.

In the following, the level scheme of ^{194}Pb will be discussed in four parts. Parts 1, 2 and 4 consist of levels feeding respectively the $I^\pi = 0^+$ ground state and the two long-lived isomeric states ($I^\pi = 11^-$, and $I^\pi = 12^+$). Part 3 corresponds to the levels connected to the dipole band denoted (d, e) in Ref. [20]. Gamma-ray transitions of each part have been selected unambiguously and most of the energy multiplets have been disentangled by analyzing four γ–γ matrices obtained with one gate on transitions of 965 keV or 280 keV (for part 1), 906 keV (for part 2), 303 keV (for part 3), and 933 keV (for part 4), thanks to the high-fold of the data.

Energies, intensities, angular distribution coefficients, and multipolarities of the transitions of ^{194}Pb deduced from this work are reported separately, for each part, in Table 1. Results of internal conversion and linear polarization measurements [8] have also been used to determine spin and parity values of some excited states.

2.1. Part 1

This part of the level scheme is shown in Fig. 1. It involves groups of transitions observed in prompt coincidence with the low-lying transitions of ^{194}Pb. The excited levels are

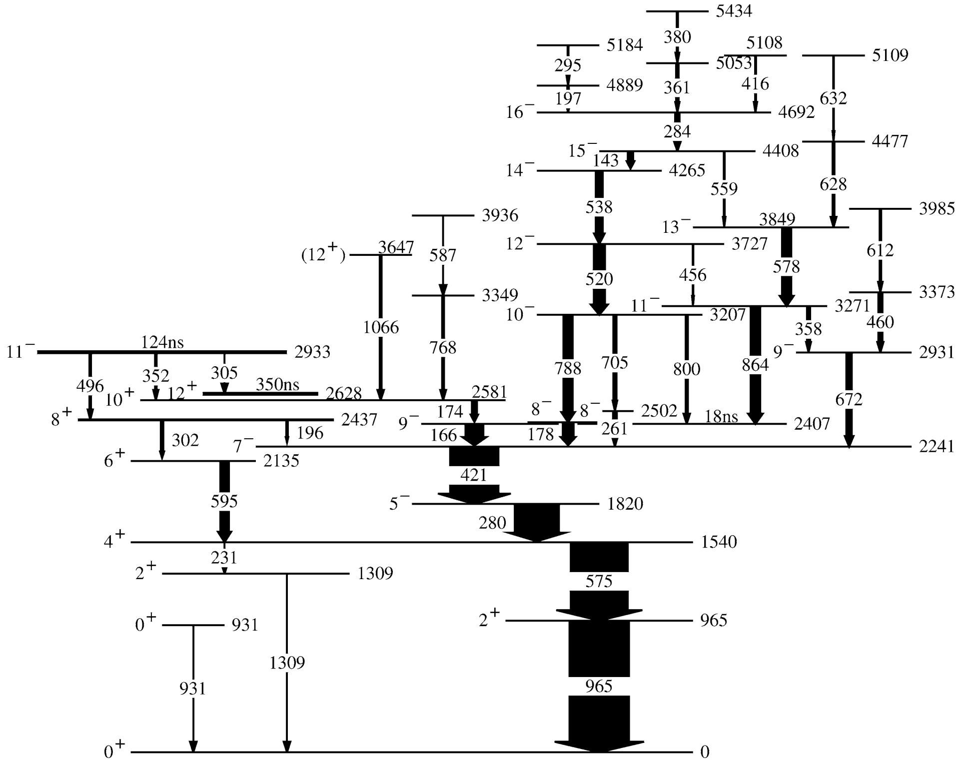

Fig. 1. Partial level scheme of ^{194}Pb (part 1) showing the transitions in prompt coincidence with the yrast 965 keV ($2^+ \rightarrow 0^+$) transition. The states $I^\pi = 0^+$ at 931 keV and $I^\pi = 2^+$ at 1309 keV have been identified in other work [27].

mainly built on the $I^\pi = 7^-$ level located at 2241 keV and exhibit irregular structures. The spin and parity of some states have been assigned from the measured values of the a_2 angular distribution coefficient: positive values have been mainly assigned to stretched E2 transitions, and negative values to stretched M1 transitions by taking into account the intensity balance of the considered states. These arguments indicate that most of the states of this group have a negative parity.

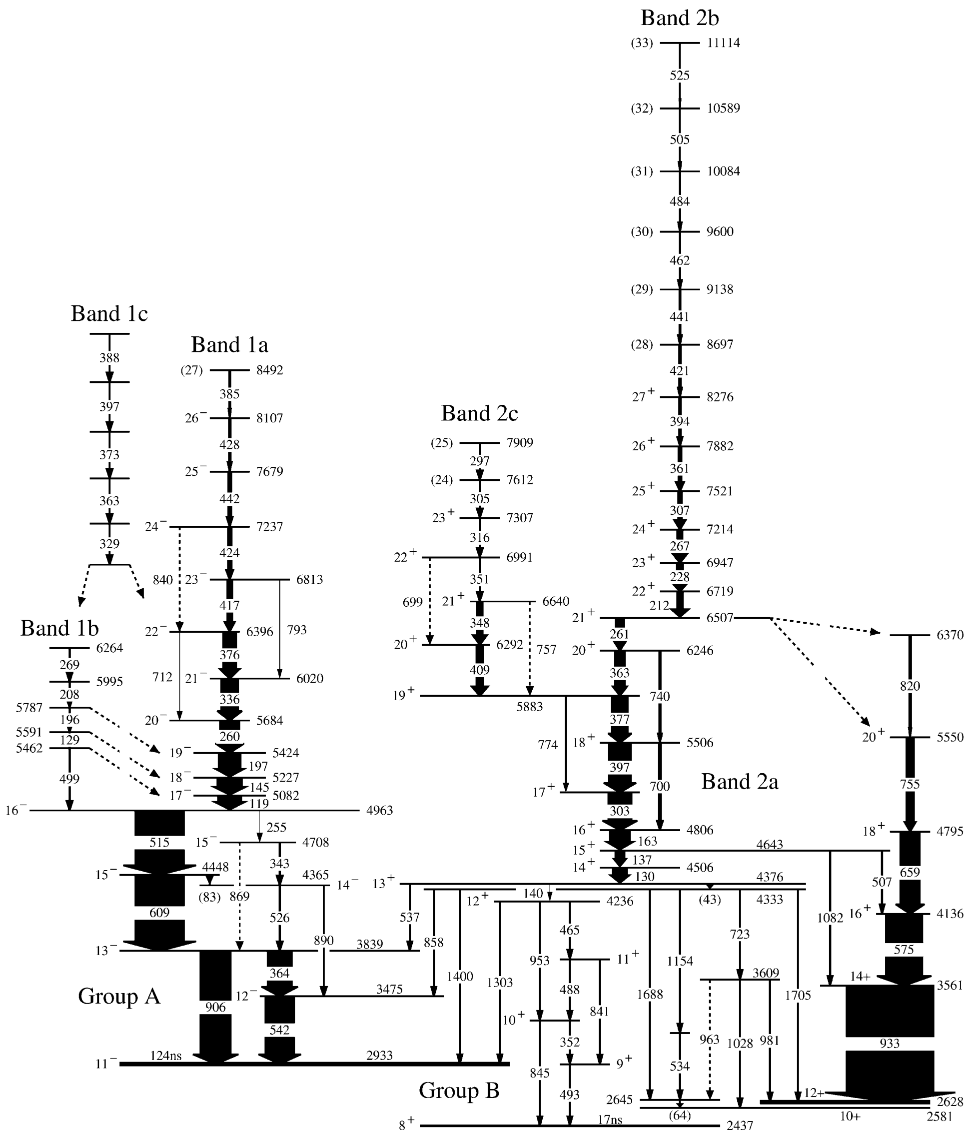

Fig. 2. Partial level scheme of ^{194}Pb (parts 2 and 3) showing several dipole structures and their decay.

2.2. Part 2

In this part (see Fig. 2) three dipole structures, called 1a, 1b and 1c, are observed to populate the level located at 4963 keV. Examples of spectra are shown in Fig. 3. The spin and parity values of this level, $I^\pi = 16^-$, have been well established from internal conversion and linear polarization measurements [8]. The levels involved in the decay of the $I^\pi = 16^-$ level towards the $I^\pi = 11^-$ isomeric state are called "group A".

Band 1a, previously known up to spin $I = 24\,\hbar$ [20,22], has been extended up to spin $I = (27)\,\hbar$ and 8.5 MeV excitation energy. Two new 712 and 793 keV cross-over transitions have been identified and the extracted values of the $B(\mathrm{M1})/B(\mathrm{E2})$ ratios are reported in Table 2. This band carries about 12% of the total intensity of the ^{194}Pb deexcitation pattern. A total of 90% of the decay intensity of the band has been measured to feed the $I^\pi = 11^-$ isomeric state (see Table 3). In addition to its main decay through the 515 keV transition, it has been found to deexcite weakly through another structure of group A which carries about 7% of the decay out of the band.

Almost all the transitions of structure 1b were previously known [21,22], except the transition of 129 keV. This structure represents 2.5% of the total intensity of the ^{194}Pb deexcitation. From double gated spectra, the two members of a doublet have been clearly identified, the 196 keV transition belongs to band 1b and the 197 keV one to band 1a.

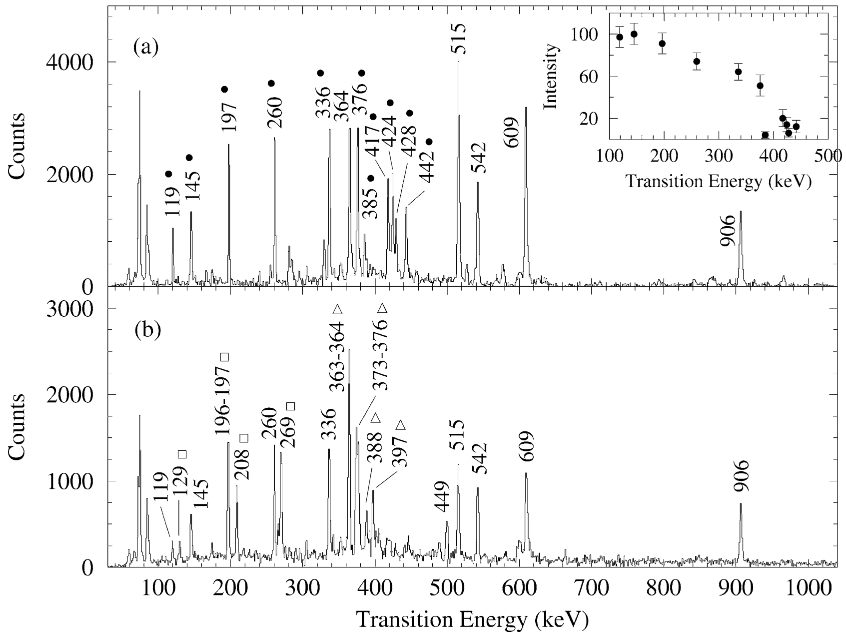

Fig. 3. Spectra of γ-rays of the dipole bands 1a, 1b, and 1c. (a) Sum of the triple-gated spectra on all the transitions of band 1a (marked with •). A small fraction of the sum of double gated spectra has been subtracted. (b) Spectrum in coincidence with the 329 keV transition of band 1c and one of the yrast transitions (609 or 906 keV). γ-lines of structure 1b are marked with □ and those of structure 1c with △.

Table 2
$B(\mathrm{M1})/B(\mathrm{E2})$ ratios calculated for several structures of ^{194}Pb

	E_γ(M1) (keV)	E_γ(E2) (keV)	$B(\mathrm{M1})/B(\mathrm{E2})^{\mathrm{a}}$ $(\mu_{\mathrm{n}}/e\mathrm{b}^2)$
Band 1a	376	712	18 (5)
	417	793	13 (3)
Band 2a	363	740	16 (3)
	377	774	18 (4)
	397	700	17 (3)
Band 3	348	636	8 (3)
	374	722	7 (3)
	397	771	6 (2)

[a] The number in parenthesis is the error in the last digit.

Table 3
Decays of the dipole bands

E_γ (keV)	$I_{\mathrm{tot}}{}^{\mathrm{a}}$
Band 1a[b]	
256	7 (2)
343	5 (1)
364	34 (2)
515	84 (5)
526	9 (2)
542	39 (3)
609	76 (5)
869	2 (1)
890	5 (1)
906	51 (3)
Band 2b[c]	
158	3 (1)
196	2 (1)
261	89 (5)
280	7 (1)
352	8 (1)
493	8 (1)
508	4 (1)
537	11 (2)
542	10 (2)
575	55 (4)
595	7 (1)
660	10 (1)
755	12 (1)
820	7 (2)
845	6 (2)
858	7 (1)
906	6 (1)
933	16 (2)
965	14 (2)
981	5 (1)
1028	3 (1)
1083	2 (1)
1154	4 (1)
1216	3 (1)
1303	4 (1)
1400	7 (2)
1688	3 (1)
1705	3 (1)
Band 3[d]	
273	15 (2)
575	15 (2)
591	33 (3)
615	22 (2)
660	22 (2)
753	33 (2)
893	16 (3)
933	69 (3)

The intensities of low-lying γ-rays coincident with bands 1a, 2b and 3 have been extracted from spectra of γ-rays in coincidence with several combinations of three γ-rays in bands 1a, 2b or 3. A small fraction of the corresponding double-gated spectra has been used for background subtraction.
[a] The number in parenthesis is the error in the last digit.
[b] Intensity normalized to the total population of the band ($I_{\mathrm{tot}}(145\ \mathrm{keV}) = 100$).
[c] Intensity normalized to the total population of the band ($I_{\mathrm{tot}}(212\ \mathrm{keV}) = 100$).
[d] Intensity normalized to the total population of the band ($I_{\mathrm{tot}}(348\ \mathrm{keV}) = 100$).

Moreover it is worth noting that the analysis of angular distributions has shown that they are both dipole transitions (Table 1) at variance to the previous measurements [21,22]. Transitions of structure 1b, above the 499 keV transition are clearly observed in coincidence with the lowest transitions of band 1a (119, 145 and 197 keV). This implies the existence of a decay path from the states of structure 1b toward the low-energy part of band 1a. However, the decay has not been identified from our data.

The new structure 1c, consisting of a cascade of five dipole transitions with similar energies, carries about 2% of the total intensity. As shown in Fig. 3, the γ-ray transitions of this structure are observed in coincidence with those of structure 1b and with those of band 1a below the $I^\pi = 22^-$ level located at 6396 keV. However, the linking transitions have not been established, only one transition of 375 keV has been clearly observed but could not be placed in the level scheme.

The $I^\pi = 16^-$ level at 4963 keV decays to the $I^\pi = 11^-$ isomeric state mainly through the known intense transitions of 515, 609 and 906 keV (group A). Another weak decay path involving the new 255, 343 and 869 keV transitions defines a new structure built on the $I^\pi = 11^-$ isomeric state. An unobserved 83 keV γ-ray transition is proposed to deexcite the $I^\pi = 15^-$ state at 4448 keV towards the $I^\pi = 14^-$ state, from the coincidence relationship observed between the 515 keV and the 526 keV transitions.

2.3. Part 3

This part comprises three dipole structures, called 2a, 2b, and 2c. Their decay spreads over many levels, called "group B" (see Fig. 2). Typical multigated spectra are shown in Fig. 4.

The level of highest excitation energy (11.1 MeV) and highest spin value (33 $\hbar$) observed in this experiment belongs to band 2b, which has been extended by six new transitions.

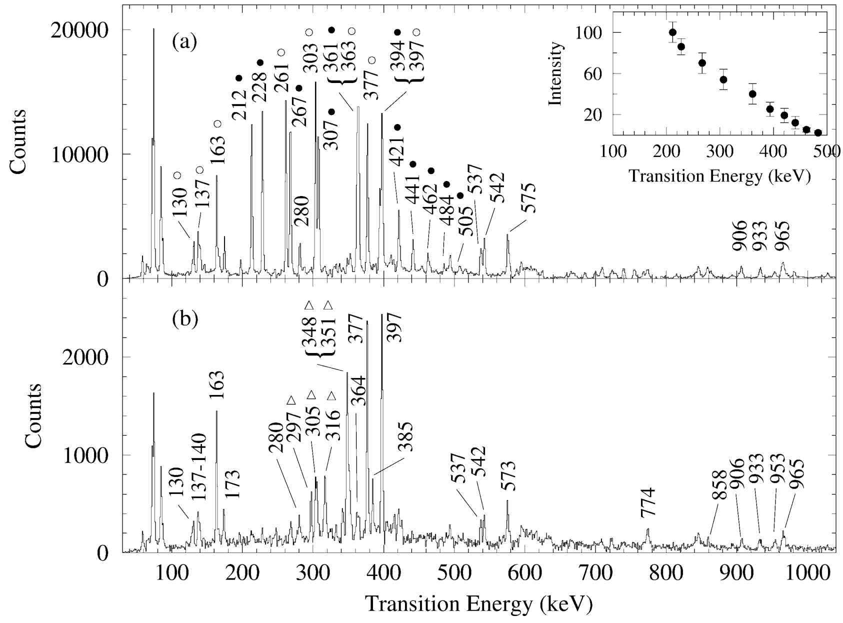

Fig. 4. Spectra of γ-rays of dipole bands 2a, 2b, and 2c. (a) Sum of the triple-gated spectra on all the transitions of band 2a (marked with ∘) and band 2b (marked with •). A small fraction of the sum of double gated spectra has been subtracted. (b) Spectrum in coincidence with the 409 keV transition of band 2c and the 303 keV transition of band 2a. γ-lines of band 2c are marked with △.

A few changes in band 2a and in its decay scheme have been made, as compared to the previous results [20,22]. The order of the 303 keV and 163 keV transitions has been reversed in order to accommodate the newly observed 700 keV cross-over transition. The 130 and 137 keV transitions have been moved down. They are placed just above the state located at 4376 keV because of their coincidence relationships with the 409 keV and 348 keV transitions which feed the $I^\pi = 19^+$ level located at 5883 keV. As previously observed [20,22], the deexcitation of band 2a is very fragmented. This part of the level scheme has also been partly modified based on new coincidence relationships observed in this experiment. Particularly, two new transitions (1082 and 507 keV) which deexcite the state located at 4643 keV have been observed to feed the known spherical states, $I^\pi = 14^+$ at 3561 keV and $I^\pi = 16^+$ at 4136 keV. Moreover, the coincidences observed with the 537 and 858 keV γ-lines which feed the $I^\pi = 13^-$ and $I^\pi = 12^-$ states located at 3839 keV and 3475 keV, respectively, define two states very close in energy which are connected by an unobserved 43 keV transition. The spin and parity values, $I^\pi = 13^+$, of the state located at 4376 keV has been determined from conversion coefficient measurements: the 140 keV transition, which connects band 2a to the known $I^\pi = 12^+$ state located at 4236 keV, is $\mathrm{M1} + \mathrm{E2}$ [8]. This result is in agreement with the values of angular distribution coefficients of several transitions de-exciting band 2a.

The $B(\mathrm{M1})/B(\mathrm{E2})$ ratios extracted in band 2a are given in Table 2. No cross-over transitions could be clearly identified in band 2b because of the existence of unresolved γ-lines which could be placed either in the band itself or in its decay scheme.

Band 2a carries about 11% of the total intensity of the reaction channel and band 2b about only 3.5%. The decay out of the $I^\pi = 21^+$ state of band 2b, located at 6507 keV, occurs mainly through the 261 keV transition which carries about 90% of the intensity of the band, the remaining 10% feeds the 6370 keV and 5550 keV spherical levels through unobserved transitions. The isomeric states $I^\pi = 11^-$ and $I^\pi = 12^+$ gather about 27% and 24%, respectively, of the total decay intensity of band 2b, while the $I^\pi = 8^+$ state located at 2437 keV collects about 14%.

Band 2c (Fig. 2) comprises four new dipole transitions of 351, 316, 305 and 297 keV observed in coincidence with the previously known 409 and 348 keV transitions which feed the $I^\pi = 19^+$ state located at 5883 keV. Two cross-over transitions of 757 keV and 698 keV have been tentatively assigned to this structure. The intensity of this structure is evaluated to be 2.5% of the total intensity of the ^{194}Pb deexcitation.

2.4. Part 4

This part (shown in Fig. 5) consists of two dipole bands, band 3 and band 4, and two groups of excited states, "group C" with positive parity and "group D" with negative parity.

Some transitions belonging to band 3 have been previously observed but ordered differently depending on authors [21,22]. From this work, they are now ordered as a regular sequence which is placed at higher excitation energy than previously proposed, taking into account several new transitions (273, 615 and 1166 keV) involved in its decay. The 591 and 753 keV transitions placed previously at high spin in this sequence [21] have been

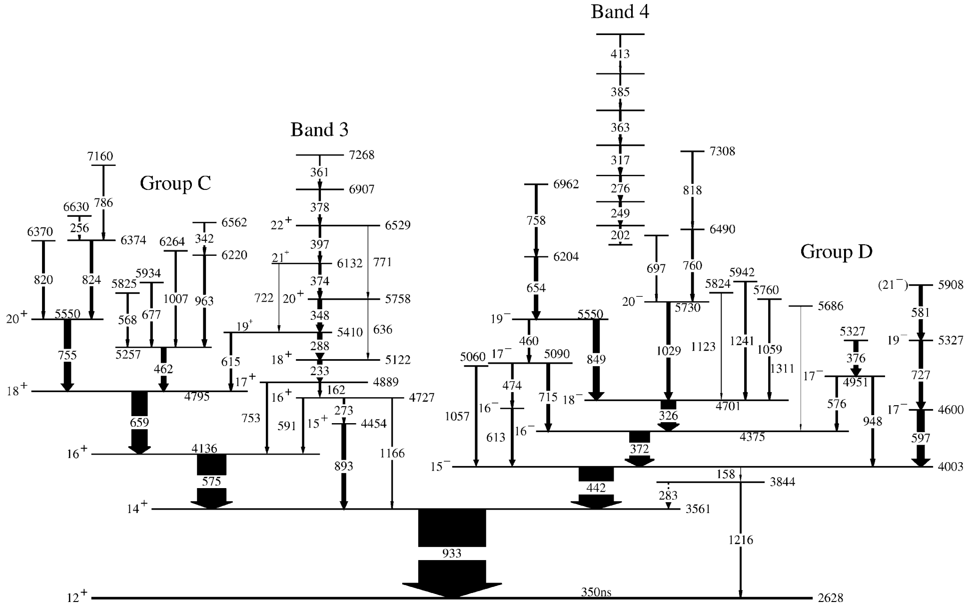

Fig. 5. Partial level scheme of ^{194}Pb (part 4) showing the excited states which feed the $I^{\pi} = 12^{+}$ isomeric state.

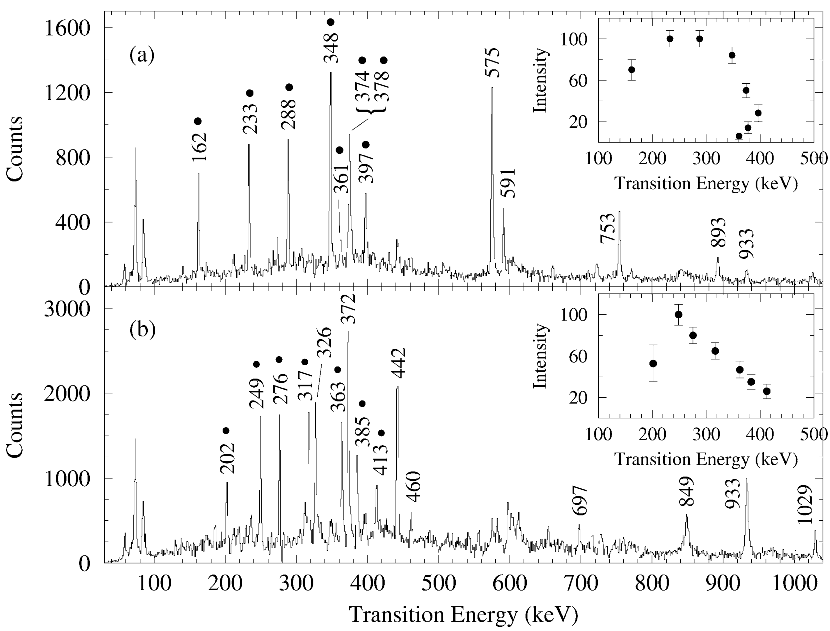

Fig. 6. Spectra of γ-rays belonging to bands 3 and 4. (a) Spectrum in coincidence with one transition of band 3 (233 or 288 keV) and the 933 keV yrast transition. The γ-lines of band 3 are marked with •. (b) Spectrum in coincidence with one transition of band 4 (249 or 276 or 317 keV) and one of the yrast transitions (326 or 442 or 933 keV). The γ-lines of band 4 are marked with •.

established to belong to its decay. Moreover, two new transitions of 378 and 361 keV energy have been added at the top of the band. The spectrum of γ transitions belonging to band 3 and its deexcitation is shown in Fig. 6. The angular distribution analysis, using double-gated spectra on few transitions of band 3, indicates that the 753 keV transition which feeds the known $I^\pi = 16^+$ state at 4136 keV and the 615 keV one which deexcites the 5410 keV state are stretched dipoles, while the 591 keV and the 1166 keV transitions have $a_2 > 0$ angular distribution coefficient. This leads to the unambiguous assignments of spin and parity to the states of band 3. New cross-over transitions have been observed and the $B(\mathrm{M1})/B(\mathrm{E2})$ branching ratios are reported in Table 2. Band 3 carries about 2% of the total intensity. Its decay-out intensity is given in Table 3. Only 70% of the total intensity of the decay has been identified.

Band 4 (see Fig. 6) has been observed for the first time in this work and consists of seven transitions, which are stretched dipoles (see Table 1). They are observed in coincidence with all the transitions which deexcite negative-parity states of “group D”, located below 6 MeV. Band 4 carries only about 1% of the intensity of the ^{194}Pb deexcitation channel. The $I^\pi = 14^+$ state located at 3561 keV gathers almost all the decay-out intensity of the band. However, the linking transitions have not been identified. This indicates that, as observed for band 2a, the deexcitation of band 4 is probably very fragmented. Contrary to the other transitions belonging to the band, the 202 keV transition is not observed in coincidence with the 597, 654, 697, 727, 849, and 1029 keV transitions, leading to an excitation energy of the band head at around 6.3 MeV with a spin value of $20 \pm 1\,\hbar$.

3. Discussion

3.1. Spherical states

Because of its closed proton shell, pure neutron excitations are first expected in the spherical nucleus ^{194}Pb. Shell-model calculations have been performed in light lead isotopes, ^{192,194,196}Pb [28]. Such calculations involving two- and four-neutron excitations have been successfully used in the interpretation of some positive and negative-parity high-spin states of ^{194}Pb (as the $I^\pi = 12^+$, $I^\pi = 14^+$, $I^\pi = 16^+$, $I^\pi = 15^-$ and $I^\pi = 17^-$ states) observed in a previous experiment [21]. The same calculations had also predicted the existence of other four-neutron negative-parity states $I^\pi = 10^-$, $I^\pi = 12^-$, $I^\pi = 13^-$ and $I^\pi = 14^-$ located at 3.26 MeV, 3.76 MeV, 4.12 MeV and 4.5 MeV, respectively, which had not been observed in that experiment. The main configurations of these states are $(9^- \otimes 2^+)$, $(9^- \otimes 4^+)$, $(5^- \otimes 12^+)$ and $(10^- \otimes 4^+)$, respectively, where the $I^\pi = 2^+$ and the $I^\pi = 4^+$ have the two quasineutron configuration $\nu i_{13/2}\nu(p_{3/2}/f_{5/2})$ and the $I^\pi = 12^+$ has the configuration $(\nu i_{13/2})^2$. These calculated states could be identified with states of part 1 observed in this work (see Fig. 1). Their excitation energy (3207, 3727, 3849 and 4265 keV) and spin and parity values agree well with the calculated energies and configurations. Two other states, $I^\pi = 11^-$ and $I^\pi = 12^+$, involving the main configurations $(9^- \otimes 2^+)$ and $(10^+ \otimes 2^+)$ have also been predicted, by the same

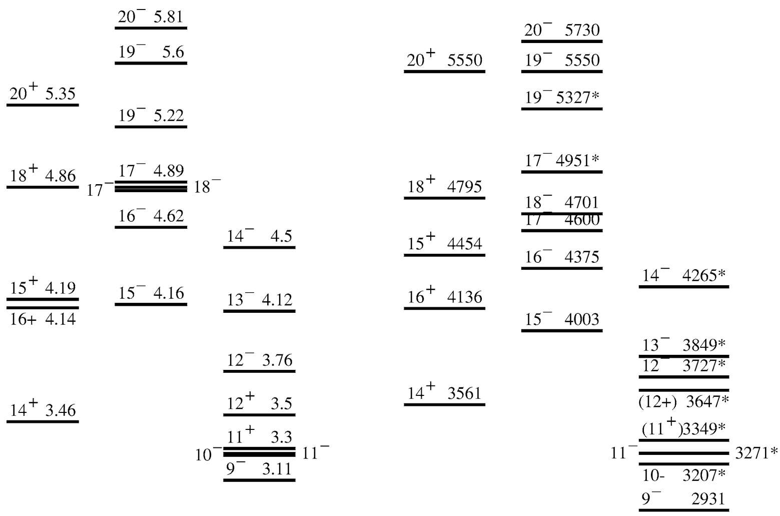

(a) : Th. (b) : Exp.

Fig. 7. Comparison of the excitation energy of the spherical four-neutron excitation states: (a) calculations [28]; (b) experiment. Newly identified states are marked with an asterisk.

calculations, at the energies of 3.3 MeV and 3.5 MeV, respectively. These states had been previously identified with states observed in [21]. However, because of some changes in the present level scheme (part 1) as compared to the previous one [21], they should rather be identified with the states located at 3271 keV and at 3647 keV, respectively. The comparison of the energies of the calculated four-neutron excitations [28] with the observed states (see Fig. 7), shows a fairly good agreement.

3.2. Multiparticle excitations and dipole bands

The numerous M1 bands already observed in the lead isotopes $^{192\text{-}202}$Pb have been extensively studied in the framework of the TAC formalism [16] (see, for example, [17] and references therein) which led to the concept of “magnetic rotation” [18]: the coupling scheme of the high-K proton particles and the high-j neutron holes giving rise to large magnetic moments, as supported by the measured B(M1) values [17]. In this section, we will only focus on the identification of the multiparticle configurations associated to the dipole bands of ^{194}Pb, as it is the sole nucleus where most of the dipole bands have been connected to the low-energy part of the level scheme.

3.2.1. Bands 1a, 2a and 2b

In our previous work [20], the configuration of the heads of the bands 1a and 2a have been proposed to be the high-K [8] two-proton state $K^{\pi} = 11^{-}$, related to a weakly-

[8] At the bottom of the bands, the K value is a good quantum number, which can be used for labeling the band-head configurations.

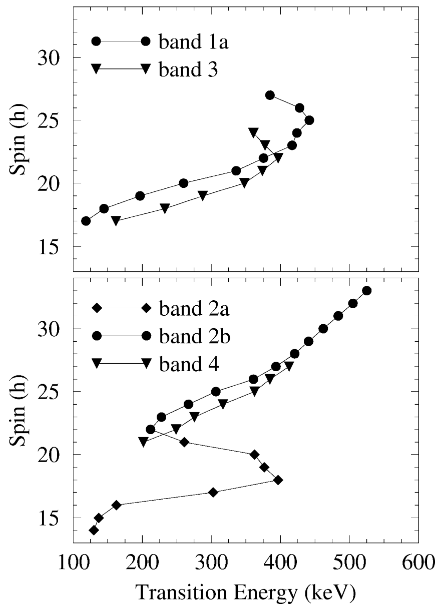

Fig. 8. Spin value, I, as a function of transition energy $E_\gamma(I \to I-1)$ for several dipole bands observed in ^{194}Pb.

deformed oblate shape of the nucleus, coupled to neutron-hole states of the high-j $\nu i_{13/2}$ subshell. The configuration assigned to band 1a was

$$\{\pi 9/2^-[505]\pi 13/2^+[606]\}K^\pi = 11^- \otimes \{(\nu i_{13/2})^2\}J^\pi = 12^+.$$

The perpendicular coupling of the proton and neutron angular momenta gives a total spin of 16 for the band head and results in a large component of the magnetic moment giving rise to large values of B(M1), as recently measured [17]. The energies of the new transitions added on the top of band 1a lead to an up-bending in the behaviour of the excitation energies of levels as a function of spin, as shown in Fig. 8. This suggests that, at about 2 MeV above the $I^\pi = 16^-$ state located at 4963 keV, another pair of $i_{13/2}$ neutrons is broken leading to a six-nucleon state with the configuration [29]

$$\{\pi 9/2^-[505]\pi 13/2^+[606]\}K^\pi = 11^- \otimes \{(\nu i_{13/2})^4\}J^\pi = 20^+.$$

The changes made both in the structure of band 2a and in its deexcitation have no implication on the previously assigned configuration [20]. The measured excitation energy, spin and parity of the I^π=13$^+$ state located at 4376 keV are in agreement with the configuration

$$\{\pi 9/2^-[505]\pi 13/2^+[606]\}K^\pi = 11^- \otimes \{(\nu i_{13/2})^1(\nu p_{3/2}/f_{5/2})^1\}J^\pi = 7^-, 8^-.$$

At higher excitation energy, the $I^\pi = 21^+$ state located at 6507 keV on which band 2b is based, can be identified as

$$\{\pi 9/2^-[505]\pi 13/2^+[606]\}K^\pi = 11^- \otimes \{(\nu i_{13/2})^3(\nu p_{3/2}/f_{5/2})^1\}J^\pi = 17^-, 18^-.$$

The extension of band 2b to higher spin [29] shows that it remains regular up to the highest spin observed, $I = 33\hbar$ (see Fig. 8).

3.2.2. *Bands 3 and 4*

Bands 3 and 4 behave like bands 1a and 2b, respectively: both bands 3 and 1a show an up-bending while bands 4 and 2b remain very regular at high spin (Fig. 8). As these behaviours are due to the different number of neutron excitations in the $\nu i_{13/2}$ subshell (respectively, 2 and 3), one can consider that the neutron excitations in bands 3 and 4 are the same as in bands 1a and 2b, respectively. As for the proton configuration, the well-identified high-K two-proton state, $\{\pi 9/2^-[505]\pi 7/2^-[514]\}K^\pi = 8^+$, can be involved in bands 3 and 4. Firstly, the excitation energy of the 1a band-head above the $K^\pi = 11^-$ state (at 2933 keV) and that of band 3 above the $K^\pi = 8^+$ state (at 2437 keV) are almost the same, 2.0 and 2.3 MeV respectively (as shown in Fig. 9). It is the same for the excitation energies of the 2b band-head above the $K^\pi = 11^-$ state as compared to that of band 4 above the $K^\pi = 8^+$ state, 3.6 and 3.9 MeV, respectively. Secondly, the $B(\mathrm{M1})/B(\mathrm{E2})$ ratios measured in these bands can be compared. The values corresponding to bands 1a and 2a are very similar (see Table 2), showing that their change as a function of the neutron configuration is weak. On the other hand, these ratios are expected to depend on the proton configuration through the value of its angular momentum along the symmetry axis (K value). Within the standard rotational model, the ratio

$$\frac{[B(\mathrm{M1})/B(\mathrm{E2})]_{K=11}}{[B(\mathrm{M1})/B(\mathrm{E2})]_{K=8}}$$

would be equal to $(K = 11)^2/(K = 8)^2 = 1.9$, assuming that the two high-K two-proton states, $K^\pi = 11^-$ and $K^\pi = 8^+$, have the same deformation and knowing that the values of the gyromagnetic factor measured for these states in the neighbouring nuclei ^{196}Pb [4] and ^{198}Po [30] are quite identical within the error bars. As the K values are expected to

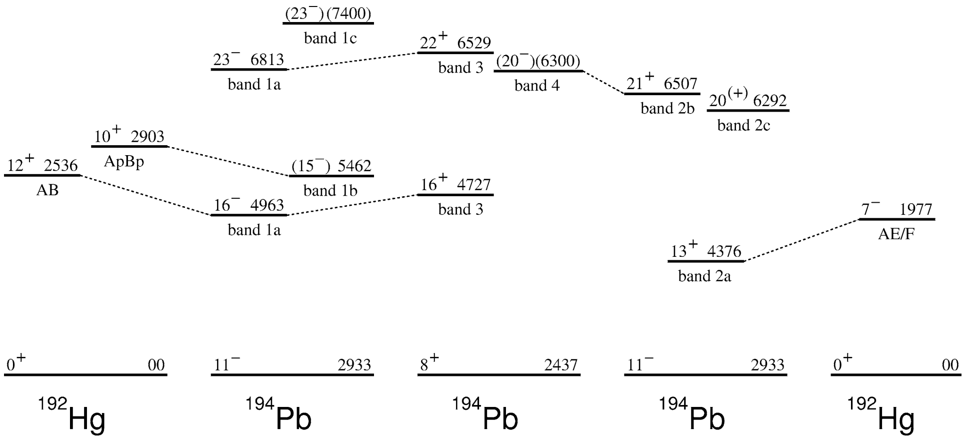

Fig. 9. Energies of all the band-head states of the dipole bands with respect to the high-K two-proton states $K^\pi = 11^-$ or $K^\pi = 8^+$. Comparison with the neutron excitations $\nu i_{13/2}$ (A, B, C, D), $\nu p_{3/2}/\nu f_{5/2}$ (E/F) and the proton excitations $\pi h_{11/2}$ ($\mathrm{A_p}, \mathrm{B_p}$) in the isotone ^{192}Hg [34,35].

remain good quantum numbers in the low part of each band, one can compare this ratio to the experimental value of the ratio for band 1a and 3, which is 2.2 ± 0.6 (see Table 2). The configurations assigned to band 3 are then

$$\{\pi 9/2^-[505]\pi 7/2^-[514]\}K^\pi = 8^+ \otimes \{(\nu i_{13/2})^2\}J^\pi = 12^+ \quad \text{at low spin,} \quad \text{and}$$
$$\{\pi 9/2^-[505]\pi 7/2^-[514]\}K^\pi = 8^+ \otimes \{(\nu i_{13/2})^4\}J^\pi = 20^+ \quad \text{at higher spin,}$$

while the configuration of band 4 is

$$\{\pi 9/2^-[505]\pi 7/2^-[514]\}K^\pi = 8^+ \otimes \{(\nu i_{13/2})^3(\nu p_{3/2}/f_{5/2})^1\}J^\pi = 17^-, 18^-.$$

3.2.3. Bands 1b and 1c

Proton excitations from the $h_{11/2}$ orbitals (with low K) may also be involved in some structures observed in ^{194}Pb. Such proton excitations have been already invoked in the ^{192}Hg isotone. The lower part of a dipole band of ^{192}Hg has been interpreted in terms of the $(\pi h_{11/2})^2(\nu i_{13/2})^2$ configuration, based on the lifetimes of some states belonging to this structure [31]. The angular momenta of the neutron and proton pairs have to be not completely aligned along the rotational axis, in order to give rise to sizeable values of the B(M1). This effect is well known in the neighbouring odd–odd Au isotopes [32,33], in which the structure corresponding to the "single" configuration $(\pi h_{11/2})^1(\nu i_{13/2})^1$ exhibits two parallel bands with different signatures, linked by strong M1 transitions, the band head having $I^\pi = 11^-$. If the angular momenta of protons and neutrons would be fully aligned, only a decoupled band of E2 transitions based on a $I^\pi = 12^-$ state would be observed in the odd–odd Au isotopes.

Moreover we can remark that the lowest-energy states of the structure of ^{192}Hg interpreted in terms of this $(\pi h_{11/2})^2(\nu i_{13/2})^2$ configuration decay towards several levels belonging to a side band extending from a $I^\pi = 22^+$ state at 6296 keV down to a $I^\pi = 10^+$ state at 2903 keV [34]. The configuration $(\pi h_{11/2})^2$ can be proposed to this latter level.

Fig. 9 shows the location of this $I^\pi = 10^+$ proton state in ^{192}Hg, as well as that of the $\{(\nu i_{13/2})^2\}I^\pi = 12^+$ neutron state. For comparison, the location of the $I^\pi = 16^-$ state of band 1a in ^{194}Pb is also reported, taking as reference the $K^\pi = 11^-$ two-proton state. As mentioned above, the $I^\pi = 16^-$ state of ^{194}Pb has the same neutron configuration as the $I^\pi = 12^+$ state of ^{192}Hg. In the same way, the state located at 5462 keV in ^{194}Pb (on which the structure 1b is based) can be related to the $I^\pi = 10^+$ state of ^{192}Hg at 2903 keV. Therefore the configuration of the band head of band 1b would be

$$\{\pi 9/2^-[505]\pi 13/2^+[606]\}K^\pi = 11^- \otimes \{(\pi h_{11/2})^2\}J^\pi = 10^+.$$

The orthogonal coupling of the two angular momenta from proton excitations, $K^\pi = 11^-$ and $J^\pi = 10^+$, gives $I^\pi = 15^-$. This is in agreement with the measured $a_2 < 0$ angular distribution coefficient for the 499 keV transition which deexcites structure 1b towards the $I^\pi = 16^-$ state located at 4963 keV. Moreover, the states of band 1b decay to the lower part of band 1a. A similar decay is also observed in ^{192}Hg, where the states built on the $I^\pi = 10^+$ level decay towards the ones having the $(\nu i_{13/2})^2$ structure [34].

Structure 1c is not connected to the lower levels, but its γ-ray transitions show clear coincidence relationships with those of structure 1b and with those of band 1a below the

$I^\pi = 22^-$ state located at 6396 keV. It is then suggested that this structure involves the same configuration as structure 1b with an additional broken neutron pair $i_{13/2}$ which is expected to occur at about 2 MeV above the $I^\pi = (15^-)$ state located at 5462 keV. The configuration that we propose to structure 1c is then

$$\{\pi 9/2^-[505]\pi 13/2^+[606]\}K^\pi = 11^- \otimes \{(\pi h_{11/2})^2(\nu i_{13/2})^2\}J^\pi = 22^+.$$

3.2.4. *Band 2c*

The $h_{11/2}$ proton excitations can also be involved in structure 2c. Indeed, as stated above, the energies needed to break one $h_{11/2}$ proton pair or one $i_{13/2}$ neutron pair are about the same (see Fig. 9). Therefore, we can expect another band head located close to the bottom of band 2b, at around 6.5 MeV excitation energy, with a spin of $I = 20\hbar$ and a positive parity. The observed $I^\pi = 20^+$ state located at 6292 keV could be identified with such a state, involving four-proton and two-neutron excitations. The suggested configuration for structure 2c is then

$$\{\pi 9/2^-[505]\pi 13/2^+[606]\}K^\pi = 11^- \otimes \{(\pi h_{11/2})^2(\nu i_{13/2})^1(\nu p_{3/2}/f_{5/2})^1\}J^\pi = 17^-, 18^-.$$

4. Conclusion

The level scheme of ^{194}Pb has been extended up to a spin of $33\hbar$ and an excitation energy of 11.1 MeV. Pure four-neutron excitations involving the spherical $\nu i_{13/2}$, $\nu p_{3/2}$ and $\nu f_{5/2}$ orbitals have been associated with the new levels connected to the $I^\pi = 7^-$ spherical state located at 2241 keV excitation energy. Most of the dipole structures observed at high spin in this work have been connected to the low-lying states. Therefore, their excitation energy, and the spin and parity values of their states have been determined. The band heads involve the high-K intruder proton states from the $\pi i_{13/2}$ and $\pi h_{9/2}$ orbitals, which drive the nucleus towards a weakly oblate shape. These two-proton excitations are coupled to several neutrons in the high-j $\nu i_{13/2}$ orbital. In this work, we have identified, for the first time in a neutron deficient lead isotope, the dipole bands involving the high-K two-proton state, $K^\pi = 8^+$, as well as the rotation-aligned proton pair, $(\pi h_{11/2})^2$. The comparison of the high-spin states in ^{194}Pb and in its isotone ^{192}Hg, involving neutron ($\nu i_{13/2}$, $\nu p_{3/2}$ and $\nu f_{5/2}$) and proton ($\pi h_{11/2}$) excitations, shows great similarities. This indicates that the yrast high-spin states of $^{194}_{82}$Pb are dominated by the coupling of the high-K two-proton states, $K^\pi = 8^+$ or $K^\pi = 11^-$, and the excitations observed in the $^{192}_{80}$Hg isotone core.

Thus, multiparticle configurations involving *all* the high-j subshells located around the Fermi levels, $\pi h_{11/2}$, $\pi h_{9/2}$, $\pi i_{13/2}$, and $\nu i_{13/2}$ have been identified in ^{194}Pb. This makes this nucleus a good candidate for simultaneous measurements of several additional quantities such as the B(M1), B(E2) and g-factors associated with the various configurations. Moreover, a similar study of high-spin states of ^{196}Pb has been undertaken in order to extend the comparative analysis of excitations in the two isotones, ^{196}Pb and ^{194}Hg [36].

Acknowledgements

The EUROGAM project was funded jointly by EPSRC (UK) and IN2P3 (France). We would like to acknowledge the technical support of the staff of the NSF (Daresbury, UK). We are especially indebted to R. Darlington of the NSF for preparing the W targets. We would like to thank Prof. H. Hübel for his comments and suggestions.

References

[1] C. Pomar et al., Nucl. Phys. A 515 (1990) 381.
[2] P. Van Duppen et al., Phys. Rev. C 35 (1987) 1861.
[3] P. Van Duppen et al., Phys. Lett. 154B (1985) 354.
[4] J. Penninga et al., Nucl. Phys. A 471 (1987) 535.
[5] J.M. Lagrange et al., Nucl. Phys. A 530 (1991) 437.
[6] J.J. Van Ruyven et al., Nucl. Phys. A 449 (1986) 579.
[7] L. Ducroux et al., Z. Phys. A 356 (1996) 241 and references therein.
[8] M. Kaci et al., Eur. Phys. J. A 3 (1998) 201.
[9] M. Kaci, PhD thesis, n° 4070, Université d'Orsay, 1996.
[10] W. Pohler et al., Eur. Phys. J. A 5 (1999) 257.
[11] J. Duprat et al., Z. Phys. A 347 (1994) 289.
[12] A.J. Kreiner, M. Fenzl, S. Lunardi, M.A.J. Mariscotti, Nucl. Phys. A 282 (1977) 243.
[13] A.J. Kreiner et al., Nucl. Phys. A 308 (1978) 147.
[14] A.J. Kreiner, Z. Phys. A 288 (1978) 373.
[15] H. Toki, H.L. Yadav, A. Faessler, Z. Phys. A 292 (1979) 79.
[16] S. Frauendorf, Nucl. Phys. A 557 (1993) 259c.
[17] R.M. Clark et al., Phys. Lett. B 440 (1998) 251.
[18] S. Frauendorf, Z. Phys. A 358 (1997) 163.
[19] A.O. Macchiavelli et al., Phys. Rev. C 58 (1998) R621, Phys. Rev. C 58 (1998) 3746.
[20] M.G. Porquet et al., J. Phys. G 20 (1994) 765.
[21] B. Fant et al., J. Phys. G 17 (1991) 319.
[22] D. Mehta et al., Z. Phys. A 345 (1993) 169.
[23] B.J.P. Gall et al., Phys. Lett. B 345 (1995) 124.
[24] A. Lopez-Martens et al., Phys. Lett. B 380 (1996) 18.
[25] I. Deloncle et al., Nucl. Instrum. Methods A 357 (1995) 150.
[26] M. Kaci et al., Z. Phys. A 354 (1996) 267.
[27] R.B. Firestone, Table of Isotopes, John Wiley, New York, 1995.
[28] N. Sandulescu et al., Phys. Lett. B 288 (1992) 235.
[29] M. Kaci et al., Act. Phys. Pol. 26 (1995) 275.
[30] A. Maj et al., Z. Phys. A 324 (1986) 123.
[31] P. Willsau et al., Z. Phys. A 355 (1996) 129.
[32] A. Neskakis, R.M. Lieder, H. Beuscher, Y. Gono, D.R. Hänni, M. Müller-Veggian, Nucl. Phys. A 390 (1982) 53.
[33] V.P. Janzen et al., Phys. Rev. C 45 (1992) 613.
[34] Y. Le Coz et al., Z. Phys. A 348 (1994) 87.
[35] H. Hübel et al., Nucl. Phys. A 453 (1986) 316.
[36] M. Kaci et al., in preparation.